

Time-domain Multitone Impedance Measurement System for Space Applications

Marc Pous

Universitat Politècnica de Catalunya
Barcelona, Spain
European Space Agency
The Netherlands
marc.pous@upc.edu

Marco A. Azpúrua

EMC Electromagnetic BCN, S.L.
Barcelona, Spain
marco.azpuru@emc-barcelona.com

Dongsheng Zhao

European Space Agency
The Netherlands
Dongsheng.Zhao@esa.int

Johannes Wolf

European Space Agency
The Netherlands
Johannes.Wolf@esa.int

Ferran Silva

Universitat Politècnica de Catalunya
Barcelona, Spain
ferran.silva@upc.edu

Abstract— This paper presents a time-domain methodology to measure the devices' live impedance at the frequency range between 30 Hz and 100 kHz. This measurement is a requirement for some space applications to ensure the stability between DC/DC converters and the onboard power. The methodology is based on a multitone excitation combined with current and voltage measurements performed with an oscilloscope. The experiments show that the measurement system obtains accurate results and offers new capabilities to deal with the drawbacks that traditional frequency-sweep instrumentation implies. The multitone approach injects signals at the entire frequency range simultaneously. Therefore, the measurement system is able to characterize time-varying and the nonlinear devices. The time-domain measurement system has been validated through different test cases achieving excellent results compared with the ones obtained using the reference impedance frequency-sweep approach.

Keywords—impedance measurements, time-domain, multitone, aerospace

I. INTRODUCTION

In some space applications, measuring the impedance of the devices connected to the power system is mandatory to ensure stability between DC/DC converters and the onboard power source. This situation is the case for the Columbus module of the International Space Station (ISS), where an impedance requirement was defined to avoid instability. The requirement between 30 Hz and 100 kHz is twofold: as long as the impedance magnitude is above the limit, the phase does not need to be considered, but as soon as the magnitude goes below the limit, the impedance phase comes into play. In such conditions, and while the the impedance phase is within limits, the requirement is still considered met. Hence, the complex impedance measurement is needed to identify and prevent instability problems.

Commonly, the abovementioned impedance measurement is performed using frequency sweep instrumentation, being the vector network analyzer (VNA) the reference system. However, the VNA and other similar impedance measurement instruments have limitations. For instance, they cannot correctly characterize time-varying or nonlinear devices because the VNA is a virtual 50 Ω environment employing calibrations [1]. Hence, impedance transformation is possible only because the measurement system and the device are linear and time-invariant.

Moreover, the VNA generates and measures single-frequency excitation signals for each frequency step. Therefore, we cannot measure harmonic distortion products generated at other frequencies employing the VNA. Other techniques combine the VNA with a power meter to overcome this problem. However, following such an approach, it is still impossible to measure the distortion products' magnitude [2], [3].

Regarding the time-variant loads, we need a measurement system capable of observing the frequency range from 30 Hz to 100 kHz with every acquisition. Otherwise, our instantaneous observation is limited to the resolution bandwidth (RBW). Furthermore, to perform an accurate measurement with the frequency sweep instrumentation, we should set the RBW to a relatively small value, implying that the sweep time increases. The RBW is small because the measurements are conducted when the test object is powered, generating noise disturbing the measurement. This setting is adequate if we measure a time-invariant load, but we can obtain highly uncertain results if the impedance changes during our measurement.

Other electric/electronic applications have to manage these difficulties [4], [5]. For example, in [4], time-varying device measurements for Power Line Communication (PLC) applications are presented. The authors use an oscilloscope at power outlets to obtain impedance measurements from the voltage and current measurements. Nevertheless, the system is based on frequency step methodology was not designed to observe the entire frequency range at once. On the other hand, in [6], a novel measurement approach based on the wideband excitation is presented for a high-speed railway application. Moreover, multitone excitation methods have been used for bioimpedance applications [7].

In that sense, bioimpedance medical applications have to cope with the time-varying impedance of the tissue properties produced by effects like breathing. Additionally, these measurement systems have to provide a high-dynamic range as the injected signal to the patient has to be weak for safety reasons. In [8], a broadband multitone excitation system is developed to measure simultaneously multiple myocardium tissue impedance. As a result, the researchers achieved high accuracy on the frequency-dependent in-vivo impedance, with a magnitude relative error lower than 1%, and absolute phase error of ± 0.3 degrees.

The work presented in our paper focuses on obtaining accurate impedance measurements with a methodology capable of evaluating the entire spectrum at each acquisition, providing the opportunity to characterize time-varying and/or nonlinear devices. Nevertheless, several concerns appear as the use of 8-bits oscilloscope instrumentation makes it challenging to achieve accurate results compared to the traditional frequency sweep instrumentation. However, in other electromagnetic interference (EMI) measurement applications, it has been demonstrated that oscilloscopes with advanced post-processing techniques can deliver accurate results compliant with CISPR 16-1-1 standard [9], [10].

Section II explains the measurement methodology, including the main considerations about synthesizing multitone excitation signals that minimize dynamic range compression, the actual setup, and the signal processing employed. In section III, different test cases are performed to validate the methodology and highlight the advantage of the multitone approach when a time-varying load is measured. Finally, the conclusions and a discussion about further work are presented in section IV.

II. METHODOLOGY

A. Multitone approach

The multitone approach can simultaneously excite the entire frequency range to ensure that the Device Under Test (DUT) meets the impedance requirements. Firstly, it is essential to build a multitone signal avoiding spectral leakage and preventing the dynamic range compression experienced when measuring broadband signals. To accomplish these objectives, it is mandatory to inject and measure periodic signals with sub-periodic tones, multiple of the primary multitone signal. Moreover, if we can generate and capture periodic signals, we can apply post-processing techniques like averaging to increase the dynamic range. On the other hand, reducing the Crest Factor (CF) of the multitone signal is crucial because it directly impacts the energy injected at each tone. Finally, our application needs to have sufficient resolution considering that we use an 8-bits oscilloscope.

Different studies deal with the CF from an analytical point of view and a numerical approach in the literature. One of the most used algorithms based on an analytical method is the method developed by Schroeder [11], which defines a solution through a simple formula to determine the initial multitone phases [12]. The initial phases of the tones to have a low crest factor are defined according to (1):

$$\varphi_k = \varphi_1 - 2\pi \sum_{i=1}^{k-1} (k-i)p_i \quad (k = 2, 3, \dots, K) \quad (1)$$

where φ_k denotes the initial phase of the k^{th} sinusoidal component in multitone, φ_1 is the initial phase of the fundamental component, K is the number of tones, and p_i is the relative power of the i^{th} component. The φ_1 value could be a random value ranging in $\pm\pi$. On the other hand, if all the tones have the same amplitude, the equation to define the initial phases can be simplified as indicated in (2):

$$\varphi_k = \varphi_1 - \frac{k(k-1)}{K}\pi \quad (k = 2, 3, \dots, K) \quad (2)$$

Other numerical methods and advanced algorithms have been created departing from the Schroeder equations to further reduce the CF. For instance, in [13], an improved CF

minimization algorithm is described, decreasing the computational time compared with other numerical approaches.

The reduction of the CF has a significant benefit on the signal-to-noise ratio of the resultant measured signal. We compute different multitone signals following different approaches and calculate their spectrum. In Fig. 1, we can observe the different time-domain signals for a multitone generated between 10 Hz and 1000 Hz with a frequency step of 10 Hz. In Fig. 1, the amplitude of the multitone signals has been normalized to compare them. This normalization is necessary because the Arbitrary Waveform Generator (AWG) limits the maximum output. Four different cases are considered:

- All the tones have the same starting phase (blue color)
- A random initial phase is selected for each of the tones (red color)
- The Schroeder algorithm is applied according to equation (2) (green color)
- The algorithm presented in [13] is considered (in black)

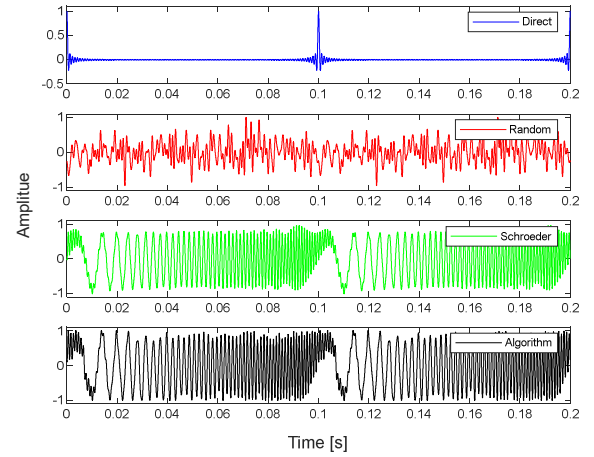


Fig. 1. Multitone time-domain comparison when the different strategies are used to compute the signal.

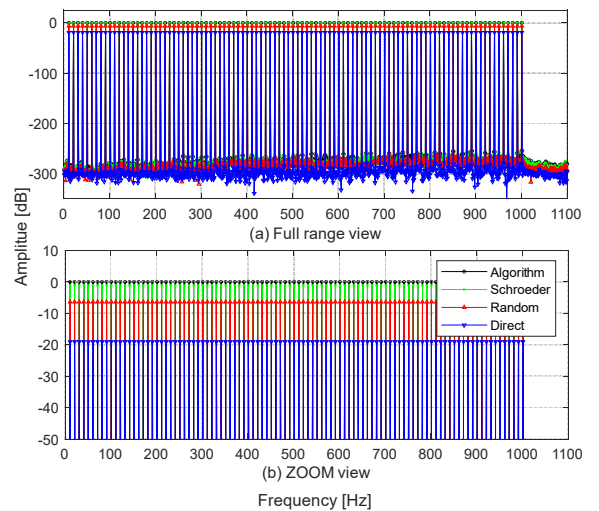


Fig. 2. Multitone frequency domain comparison when the different strategies are used to compute the signal.

In Fig. 2, the spectrum of the different multitone signals is compared. With the periodic multitone created using MATLAB®, we can clearly identify the frequency bins. Otherwise, we observe that depending on the phases of the multitone, we achieve different amplitude levels. To have the highest signal level at each frequency bin it is vital to overcome the limitations of the AWG, the coupling losses of the injecting system, and the 8-bits scope. Finally, in TABLE I, the different generated excitation signals are compared.

TABLE I. MULTITONE COMPARISON EMPLOYING DIFFERENT METHODS TO COMPUTE THE INITIAL PHASES

Multitone comparison		
Reference	Crest Factor (CF)	Spectral Difference
Algorithm ^a	1.76	0 dB
Schroeder	1.99	-1.1 dB
Random phase	4.2	-6.4 dB
Direct (in-phase)	59.6	-19.1 dB

^a. Applying the algorithm described in [13]

As the difference between the algorithm in [13] and Schroeder cases is close to 1 dB for the study case, we decided to use the Schroeder approximation with little computational cost because we can change parameters on the fly at the software. At the measurements results obtained in the next section, it is clear that we reach sufficient accuracy on the final measurement with this approach. However, some multitone can be created and stored before the campaign for future measurements. On the other hand, we can discard the direct computation and the random phase from the spectral analysis as they have a noticeable reduction in the energy injected at each of the tones.

B. Measurement procedure

The measurement procedure can be summarized as follows. Firstly, we generate the signal that will excite the measurement system considering the CF, frequency resolution, amplitudes, and signal periodicity. Then, we measure the signal injected at the DUT port that is the differential voltage and the current at the terminals of the DUT using time-domain instrumentation. We acquire full periods of the signal using the same time-base between the scope and the AWG to apply techniques like averaging the different periods of the primary multitone signal. Next, we compute the Discrete Fourier Transform (DFT), focusing on the frequency bins where we know a tone stimulates the measurement system. The final step is to compute the complex impedance, considering the correction factors of the current probe and the differential voltage probe.

Fig. 3 shows the schematic for the measurement setup. We can observe the AWG Tabor Electronics model WW1281 synthesizing the multitone signal coupled to the DUT. To inject the signal, we employ a Hubert A 1110-16-A Amplifier and a Solar electronics model 6220-2 isolation transformer. To measure the voltage and current to compute the impedance, we use Pearson 1110-A current probe and the Agilent differential voltage probe 1141A. Finally, the Tektronix DPO7254 Oscilloscope captures the time-domain signal controlled by a standard laptop through an ethernet connection.

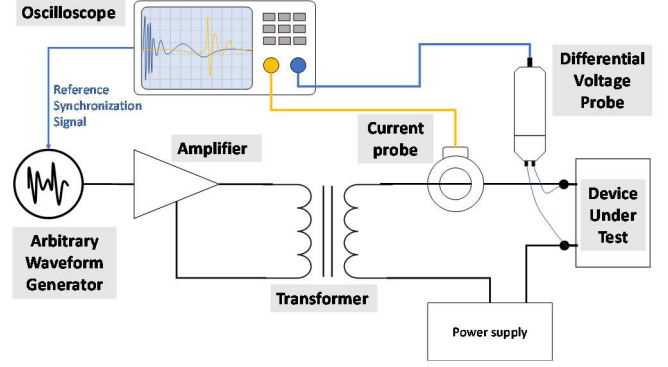


Fig. 3. Impedance measurement test setup applying the time-domain multitone methodology.

A MATLAB® application has been developed to create the multitone signal on the fly, set the AWG and the measurement scope to the proper settings, acquire the measured signals to compute the impedance, and store and plot the impedance. The application allows us to select the total measurement time as multiples of the primary frequency of the multitone signal. These capabilities allow us to quickly define the total measured time and deal with time-varying impedance devices. If the impedance is not varying in this measurement time, we can get the complete spectral response of the measuring device. Therefore, we can state that we are obtaining full-frequency instantaneous measurements.

The period of the multitone signal determines the cycle of the lowest frequency component or the step between frequencies, which is lower. Therefore, it is imperative to capture full periods of the multitone to avoid spectral leakage impacting the accuracy of the measurement. Otherwise, we shall acquire several periods to apply waveform averaging that increase the exactitude of the measurement. Therefore, the measurement time shall be defined by the minimum frequency or the frequency step and the averaging of the multitone signal. For example, if the lowest frequency is 10 Hz and we want to average at least ten periods, we need to capture 1 s during the measurement. Conversely, if we define a 100 Hz resolution between tones and want to average 25 periods, we need to store 250 ms. On the other hand, if we measure a time-varying device, we shall limit the observation time, playing with the frequency resolution and the averaged cycles.

Finally, other concern regarding this methodology is if it can deliver accurate results compared to traditional methodologies employing the 8 bits oscilloscope in combination with the arbitrary generator and the nonlinear power amplifiers. Therefore, in the next section, comparisons between the time-domain method employing the oscilloscope and measurements carried out with frequency sweep instrumentation are made to determine if the developed method is accurate and suitable to be used for this application.

III. RESULTS

To validate the time-domain methodology, we compare different measurements in this section. First, we compare a purely resistive load for validation purposes and different power converters applied in the sector. Finally, we use a programmable electronic load to measure time-varying impedance devices and to demonstrate the system's capability.

The reference measurement method employs the 4395A Network/Spectrum/Impedance Analyzer. The measurement method applies the same injection method and measurement

probes as described in Fig. 3. The difference is the use of the radiofrequency tracking generator as the input of the amplifier, and the probes are connected to the two different inputs of the impedance analyzer. To perform accurate measurements in the frequency range between 30 Hz and 100 kHz, we create a sweep table with RBW varying from 1 Hz and 10 Hz and with a total sweep time of 247 s.

A. Measurements Validation

The test object to validate the developed methodology is a resistive load. This passive $30\ \Omega$ load is commonly employed to verify the measurement procedure just-before-test. On this occasion, we are using the verification device to compare the data obtained with the reference impedance analyzer and our methodology.

The excitation signal is a multitone from 30 Hz to 100 kHz. The data obtained at the oscilloscope is shown in Fig. 4. In this Figure, we can see that channel 1 (CH1) is the response of the differential voltage probe, and channel 2 (CH2) is the signal provided by the current probe. Hence, it is essential to highlight the low amplitudes measured. Nevertheless, the signal acquired combined with the post-processing techniques is sufficient to obtain accurate results, as we see in the impedance's results.

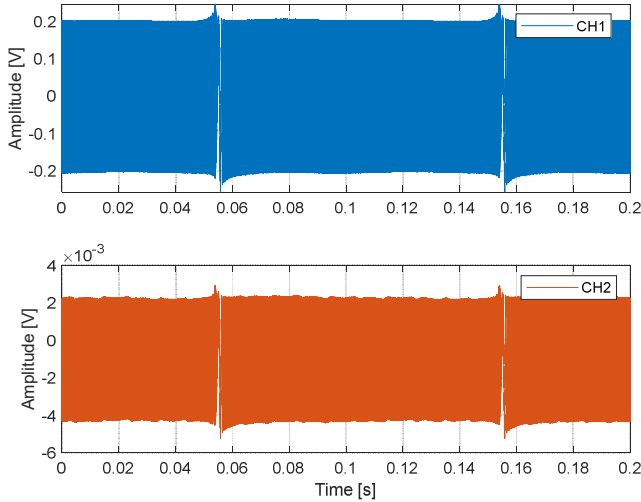


Fig. 4. Time-domain acquisitions made with the oscilloscope when the $30\ \Omega$ resistor was measured. CH1 is the output of the differential voltage probe and CH2 is the output of the current probe before the unit correction.

After applying the post-processing, we obtain the results shown in red color in Fig. 5. We are comparing the impedance's magnitude Fig. 5 (a) and phase Fig. 5 (b) with the reference instrument (blue). The results show the $30\ \Omega$ load results, where we observe a slight inductive performance due to the non-ideal characteristics of the resistor.

The results show excellent agreement between the results obtained with the VNA method and the time-domain approach. Furthermore, the magnitude relative difference is lower than 2.5 %, and the absolute phase difference is lower than one degree. Therefore, the multitone measurements carried out with the 8-bits scope produce accurate results for our application. Specifically, if we consider the advantages that measuring the entire spectrum at each capture brings us.

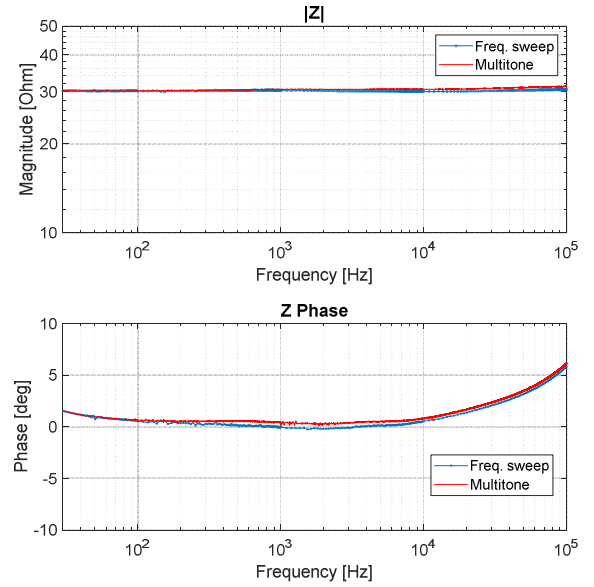


Fig. 5. Impedance results obtained when the $30\ \Omega$ is measured. In blue using the impedance analyzer and in red using the time-domain methodology.

B. Power Converters Measurements

Once the methodology has been validated with the resistive load, we perform impedance measurements on real test cases. For this purpose, we carry out measurements on different power converters applied in the GAIA mission. Our test dummy can be set with different input filters, thus varying the impedance of the DUT.

Fig. 6 shows the result using the frequency sweep instrumentation in blue and in red when the developed approach is employed. We observe an excellent fitting at the impedance's magnitude and phase. The magnitude varies from $30\ \Omega$ to less than $0.1\ \Omega$, and we can obtain accurate data as it is done with the reference frequency-sweep instrumentation.

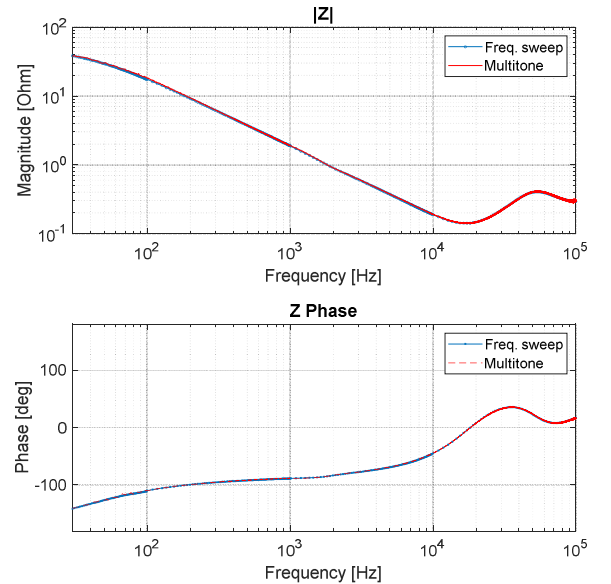


Fig. 6. Impedance results obtained when the GAIA converter with reference CGDM-J-5-0-0 is measured. In blue using the impedance analyzer and in red using the time-domain methodology.

In Fig. 7, we can observe other results obtained to our test object when a converter from Advanced Analog is used. The impedance measurements obtained for an Interpoint converter are shown in Fig. 8. For the cases in Fig. 7 and Fig. 8, we are also placing an EMI filter observing the impact on the impedance measurement. The data shows that the time-domain methodology can get equivalent results as the impedance analyzer. Furthermore, the different datasets fit all the test cases evaluated, presenting minor differences insignificant for our purpose. Nevertheless, once it has been demonstrated that the methodology is working correctly and gets satisfactory results, a further study on the measurement error and accuracy is desirable.

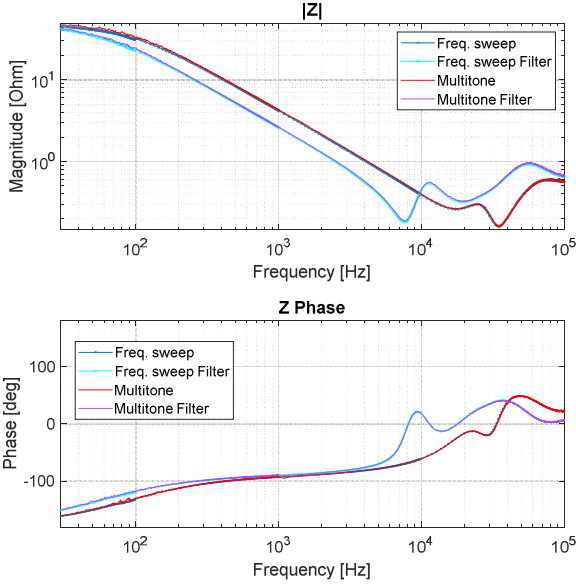


Fig. 7. Impedance results obtained when the Advanced Analog ATR2805S device is measured. In blue using the impedance analyzer and in red using the time-domain methodology when no filter is placed. In cyan and magenta, when the AFV461 filter is employed.

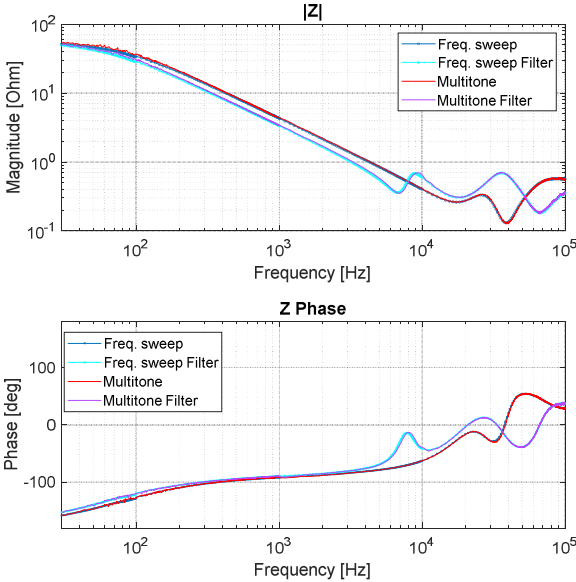


Fig. 8. Impedance results obtained when the Interpoint MTR2805S device is measured. In blue using the impedance analyzer and in red using the time-domain methodology when no filter is placed. In cyan and magenta, when the FMC28-461 filter is employed.

C. Time-Varying Load Measurements

The last study case applies to a time-varying impedance test object. For validation purposes of the methodology, we employ a controlled electronic load. The benefits of using the electronic load are that it is stable and it can be programmed to have repetitive impedance cycles. The electronic load used for the measurements is the Agilent Electronic Load model N3301A.

We define three impedance values: 10 Ω , 100 Ω , and 1000 Ω . The electronic load is commuting between them every 10 s.

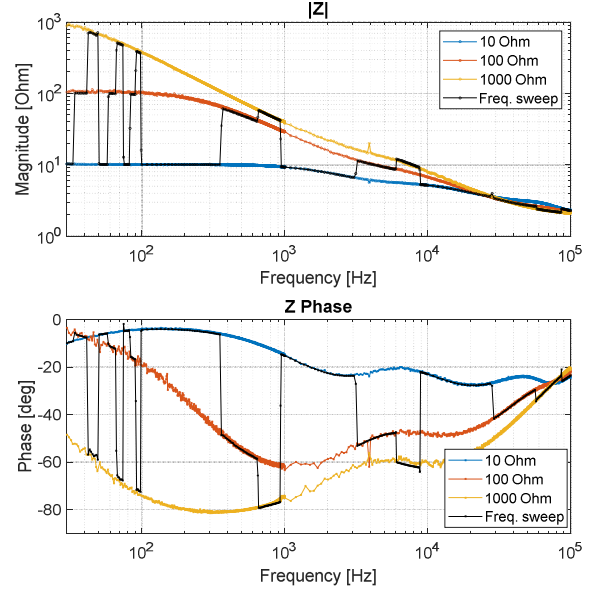


Fig. 9. Impedance results obtained when the time-varying electronic load is measured. In black using the impedance analyzer and in blue, red and yellow using the time-domain methodology.

The first measurement that we conduct employs the VNA method. In Fig. 9, in black, we see the result obtained with the impedance analyzer, where we can observe discontinuities that coincide with impedance changes and the sweep time. As the complete measurement takes 247 s, we observe abrupt changes in the trend of the measured impedance that produce incorrect results. It is nearly impossible to reach proper conclusions if we do not know the device's performance beforehand. Alternatively, we can get the complete spectrum response by employing the time-domain methodology with multiple captures. The short measurement time makes it feasible to characterize the three different impedance responses of the electronic load. In Fig. 9, we plot all the impedance responses for the pre-defined values. It is essential to clarify that the impedance has three curves corresponding to the three different impedance settings selected. The electronic load is not purely resistive, changing its impedance with frequency. Furthermore, the results obtained with the impedance analyzer fit within one of the three curves obtained with the time-domain approach.

IV. CONCLUSIONS

The results presented in this paper demonstrate that it is feasible to employ the time-domain methodology to obtain accurate impedance measurements. Moreover, the

methodology that uses a multitone broadband excitation permits overcoming some of the drawbacks that standard frequency methodology implies, specifically for time-varying impedance or nonlinear devices. Among the excellent impedance results obtained with the 8-bits scope, the time-varying electronic load highlights the possibilities of full-spectrum measurements compared to the frequency sweep implementation.

These new capabilities of the measurement system are a good advantage for the space application, where finding the worst-case scenario is mandatory to avoid malfunctions that can lead to mission failures.

Nevertheless, the study of the measurement system shall continue to define the measurement error, accuracy, and uncertainty budget of the time-domain impedance system. Evaluating the impact of using other instrumentation or the number of cycles necessary to provide sufficient accuracy is necessary. Finally, the measurement of nonlinear loads has to be completed considering aspects such as the injected multitone signal level because it can produce different system responses.

ACKNOWLEDGMENT

The project on which these results are based has received funding from the European Union's Horizon 2020 research and innovation programme under Marie Skłodowska-Curie grant agreement No. 801342 (TecniospringINDUSTRY) and the Government of Catalonia's Agency for Business Competitiveness (ACCIÓ).

This work was supported by the Spanish "Agencia Estatal de Investigación" under project PID2019-106120RB-C31/AEI/10.13039/501100011033.

REFERENCES

- [1] K. A. Remley, "Practical applications of nonlinear measurements," *2009 73rd ARFTG Microwave Measurement Conference*, 2009, pp. 1-15, doi: 10.1109/ARFTG.2009.5278060.
- [2] D.C. Kerr, J.M. Gering, T.G. McKay, M.S. Carroll, C.R. Neve, and J.-P. Raskin, "Identification of RF harmonic distortion on Si substrates and its reduction using a trap-rich layer," *IEEE Radio and Wireless Conf.*, pp. 151-154, Jan. 2008.
- [3] J. Dunsmore, "Novel method for vector mixer characterization and mixer test system vector error correction," *IEEE MTT-S Int. Microwave Symp. Dig.*, vol. 3, pp. 1833-1836, Jun. 2002.
- [4] M. Antoniali and A. M. Tonello, "Measurement and Characterization of Load Impedances in Home Power Line Grids," in *IEEE Transactions on Instrumentation and Measurement*, vol. 63, no. 3, pp. 548-556, March 2014, doi: 10.1109/TIM.2013.2280490.
- [5] G. Hallak, C. Nieß and G. Bumiller, "Accurate Low Access Impedance Measurements With Separated Load Impedance Measurements on the Power-Line Network," in *IEEE Transactions on Instrumentation and Measurement*, vol. 67, no. 10, pp. 2282-2293, Oct. 2018, doi: 10.1109/TIM.2018.2814138.
- [6] P. Pan, H. Hu, Z. He and Y. Li, "Rapid Impedance Measurement Approach Based on Wideband Excitation for Single-Phase Four-Quadrant Converter of High-Speed Train," in *IEEE Transactions on Instrumentation and Measurement*, vol. 70, pp. 1-11, 2021, Art no. 9004611, doi: 10.1109/TIM.2021.3107048.
- [7] B. Sanchez, J. Li, T. Geisbush, R. Bragos and S. B. Rutkove, "A pilot spectroscopy study on time-varying bioimpedance during electrically-induced muscle contraction," *2014 36th Annual International Conference of the IEEE Engineering in Medicine and Biology Society*, 2014, pp. 3739-3742, doi: 10.1109/EMBC.2014.6944436.
- [8] B. Sanchez, J. Schoukens, R. Bragos and G. Vandersteen, "Novel Estimation of the Electrical Bioimpedance Using the Local Polynomial Method. Application to In Vivo Real-Time Myocardium Tissue Impedance Characterization During the Cardiac Cycle," in *IEEE Transactions on Biomedical Engineering*, vol. 58, no. 12, pp. 3376-3385, Dec. 2011, doi: 10.1109/TBME.2011.2166116.
- [9] M. A. Azpúrua, M. Pous and F. Silva, "Statistical Evaluation of Measurement Accuracy in Full Time-Domain EMI Measurement Systems," *2020 International Symposium on Electromagnetic Compatibility - EMC EUROPE, 2020*, pp. 1-6, doi: 10.1109/EMCEUROPE48519.2020.9245837.
- [10] M. A. Azpúrua, M. Pous and F. Silva, "Specifying the Waveforms for the Calibration of CISPR 16-1-1 Measuring Receivers," in *IEEE Transactions on Electromagnetic Compatibility*, vol. 62, no. 3, pp. 654-662, June 2020, doi: 10.1109/TEM.2019.2923813.
- [11] Schroeder, Manfred R.. "Synthesis of low-peak-factor signals and binary sequences with low autocorrelation (Corresp.)." *IEEE Trans. Inf. Theory* 16 (1970): 85-89.
- [12] J. Schoukens, R. Pintelon, E. van der Ouderaa and J. Renneboog, "Survey of excitation signals for FFT based signal analyzers," in *IEEE Transactions on Instrumentation and Measurement*, vol. 37, no. 3, pp. 342-352, Sept. 1988, doi: 10.1109/19.7453.
- [13] Yang, Yuxiang & Zhang, Fu & Tao, Kun & Sanchez, Benjamin & Wen, He & Teng, Zhaosheng. (2015). An improved crest factor minimization algorithm to synthesize multisines with arbitrary spectrum. *Physiological Measurement*. 36. 10.1088/0967-3334/36/5/895.